

PACS numbers: 06.30.Bp; 07.60.–j; 42.55.Lt; 42.60.Da
DOI: 10.1070/QE2013v043n02ABEH015045

Development of precision laser goniometer systems*

M.N. Burnashev, P.A. Pavlov, Yu.V. Filatov

Abstract. **The concept of constructing precision laser goniometer systems, based on integrating a ring laser and an optical angle sensor with the holographic principle of angular scale recording is considered. The concept implies the application of the cross-calibration procedure, aimed at determination of systematic components of the errors of angle sensors, used in the system. The results of the presented system studies demonstrate the error of angular measurements amounting to ~0.01″. The results of implementing the proposed concept in the creation of a standard system of the plane angle unit of rigid rotation and the measuring and computing complex for automated control of digital angle transducers with high digit capacity are briefly presented.**

Keywords: *ring laser, angle measurements, cross-calibration, angle transducer, optical angle sensor.*

1. Introduction

The analysis of development of precision systems for angular measurements shows that, alongside with the accuracy of the measurements, the resolving power becomes a characteristic of primary importance [1]. While at the previous stage of development in a majority of angle-reproduction systems use was made of rotary tables with two autocollimators and a polyhedral prism, or a Moore table with an autocollimator and a polyhedral prism, at present one can observe conversion to tables with optical angle sensors (OASs) with typical division value of the order of 30″ (without interpolation of the output signal phase). Application of the interpolation technique reduces the division value to a few hundredths of arc second. In many cases (e.g., in the angular comparator, developed at Physikalisch-Technische Bundesanstalt (PTB), Braunschweig, Germany [2]) they use OASs, specially designed for these systems and having the division value of the order of a few arc seconds. Designing OAS-based systems allows complete automation of the angle reproduction process and achievement of the setup resolving power at the level of hundredths and thousandths of arc second by using the interpolation of the OAS output signal.

*Reported at the 'Laser Optics' conference (St. Petersburg, Russia, June 2012).

M.N. Burnashev, P.A. Pavlov, Yu.V. Filatov Saint Petersburg Electrotechnical University 'LETI', ul. Prof. Popova 5, 197376 St. Petersburg, Russia; e-mail: yvfilatov@mail.eltech.ru

Received 24 October 2012; revision received 14 November 2012.
Kvantovaya Elektronika **43** (2) 130–138 (2013)
Translated by V.L. Derbov

The systems of such type essentially better satisfy the requirements of unifying the measurement process, since high-accuracy and high-sensitivity OASs find more and more applications in industry and enginery. It is important that a number of angle transducers operate both in static regime (for measuring the constant angle values) and in dynamic regime (for measuring the time-dependent angle values), and some of the transducers are intended for operation in the dynamic regime only. This gives rise to the necessity of extending the functional capabilities of measuring systems, namely, they should provide angle measurements both in static and dynamic regimes.

The use of the dynamic laser goniometric method [3, 4] allows both the calibration of plane-angle measuring instruments, operating in the dynamic regime, and highly productive, economically efficient calibration of some instruments for constant plane angle measurements.

The principle of laser goniometer operation is based on the use of a ring laser (RL), rotating with a quasi-constant velocity and playing the role of an etalon angular limb with extremely high resolution and uniformity of the sequence of scale marks. The use of this method provides the most favourable conditions for attaining extreme accuracy characteristics. The measurement technologies, used in the modern laser dynamic goniometry, allow estimation of its potential accuracy, determined by quantum fluctuations of the RL output signal**, at the level of a few thousandths of arc second [4].

The results of the studies have shown that the major sources of random errors are quantum and broadband technical fluctuations of the RL output signal. Usually, the maximal value of the dispersion of these errors does not exceed $(0.0025'')^2$, i.e., the root-mean-square deviation $\sigma < 0.05''$. It is worth noting that the presented value corresponds to the error of a single measurement, i.e., the measurement, performed during one revolution of the base, the period of which usually falls within the range from 1 to 3 s. Further reduction of the random error in the laser goniometer is possible at the expense of acquisition and statistical processing of large arrays of measurement results, which is easily implemented in the dynamic regime. Hence, the random measurement error amounts to a few thousandths of arc second, provided that the measurement data array is large enough.

The systematic error of the angle measurement, using the RL calibration within the angle 2π, is caused, first of all, by the periodic variation of the RL parameters under the action of a certain factor. One of the most essential sources of the

** In the present paper we discuss the use of ring lasers for angle measurements; therefore, below we consider the ring laser as a measuring transducer of angular displacement.

RL systematic error is the action of a permanent external magnetic field (e.g., the magnetic field of the Earth). The RL possesses a certain axis of sensitivity to the magnetic field, lying in its cavity plane [5]. In the course of rotation, the sensitivity axis changes its orientation with respect to the force lines of the magnetic field, which leads to a systematic error at the first harmonic (provided that the magnetic field is uniform) of the rotation frequency. This component of the error can be taken into account and compensated algorithmically.

Another source of the RL systematic error is the instability of its angular velocity. In this case equal angular intervals are passed during unequal time intervals. Since the RL is an inertial sensor, i.e., it is sensitive to angular displacements with respect to an inertial frame, the rotation of the Earth creates an additive contribution to the frequency of its output signal. Being integrated over time intervals that are larger or smaller due to unstable rotation velocity, this contribution produces systematic distortions of the angular scale of the RL. The use of the algorithms of the phase-temporal method [6] allows practical elimination of the systematic RL error, caused by the instability of rotation velocity and the shift of zero of the output RL characteristic.

2. The concept of constructing precision laser goniometer systems

The obtained results demonstrate that the dynamic goniometer based on the RL is a measuring system of extremely high accuracy. The RL implements the angular scale based on the harmonic structure of the electromagnetic field in the closed optical resonator. Due to this fact, the RL as an angle transducer is characterised by super-high resolution and unprecedented scale uniformity. At the same time, the scale factor of the RL and, therefore, the division value of its angular scale are subject to some temporal variations, which makes it necessary to perform current calibration of the RL within the angle 2π or other angles, known in advance. These specific features of the RL determine the reasonability of its integration with angle transducers on the base of essentially different physical effects, when constructing high-accuracy laser goniometric systems.

As a transducer of such kind one can use OASs, providing essentially less uniform, but, nevertheless, temporarily more stable scale. OASs find wide applications in precise mechanical engineering, measurement technology, and metrology. Modern technologies allow manufacturing of angular scales with non-uniformity of the order of a fraction of arc second. The application of interpolators of the signal, reducing the discreteness of readings, and the use of the methods, compensating the OAS systematic error, allow creation of OAS-based angle-measuring systems with the error of the order of hundredths of arc second. In this case, specially designed angular scales having large diameter and, therefore, large number of graduation marks, are used. Thus, the angular scale, used in the angular comparator in PTB, has the diameter 40 cm and the number of graduation marks 262144 [2]. Among OASs a special place is occupied by the devices with the angular scale, produced on the base of holography principles [7]. Such scales are characterised by high uniformity, small dimensions and high resolution. Its use allowed creation of a number of high-accuracy angle-measuring systems.

In Table 1 the basic characteristics of RLs and OASs are presented for comparison. Different character of the random component of the error and the spectral composition of systematic errors, as well as different physical principles of the angle scale formation, give rise to new possibilities for combining RLs and OASs and creating high-accuracy angle-measuring systems on their base.

Besides the advantages, mentioned above, the presence of two angle transducers in one measuring system allows implementation of the cross-calibration procedure, providing determination of systematic components of the errors from both transducers. The cross-calibration procedure [8] consists in performing step-by-step calibration of one transducer using the other one (usually this is a transducer with a higher resolving power). After each step of the calibration procedure, the frame (stator) of one transducer is rotated through the angle $360°/n$ with respect to the other one, where n is the number of the cross-calibration steps. As a result, one gets an $n \times n$ data array, the processing of which allows obtaining systematic components of the errors of both transducers. The number of revolutions n (or the minimal angle of rotation $360°/n$) is an important factor in performing the cross-calibration procedure. The maximal-order harmonic of the systematic error, which can be determined by means of cross-calibration, is the harmonic with the number $n/2$.

At large n the classical method of cross-calibration becomes very laborious. At present the methods for analysing the systematic error in angle sensors using the Fourier transform are developed [9–12]. All these methods imply exploitation of two or more similar sensors, except the method of self-calibration [13, 14], used for error analysis in the PTB angular comparator. However, the self-calibration method requires mounting multiple recording heads, distributed around the circle with angle separation, multiple of $2n$. Due to the specific features of the OAS angular scale, the integration of RLs with OASs offers the possibility of using the modified method of cross-calibration [15].

Using these considerations, we developed the concept of constructing a high-accuracy laser goniometer system, implying the use of the following measuring angle transducers:

1. The single-block ring He-Ne laser GL-1 having the perimeter 0.4 m, which corresponds to the scale factor $\sim 10^6$ or the resolution $1.3''$ pulse^{-1}.

2. An OAS, represented by the holographic photoelectric angle transducer PKG-105M. Its scale is produced using holographic methods and contains 324000 scale labels per complete revolution (the resolution of $4''$ pulse^{-1}).

3. The polyhedral prism (PP) in combination with the optical null indicator (NI).

Table 1. Basic characteristics of ring lasers and OASs.

Device	Characteristic		
	Uniformity of angular scale	Random error	Systematic error
RL	Super-high	Depends on the velocity of rotation and the measured angle	Low-frequency components dominate in the spectrum (no special requirements to the rotation axis mounting)
OAS	Moderately high	Independent of the rotation velocity and the angle measured	Presence of high-order harmonics in the spectrum (high requirements to the rotation axis mounting)

The block diagram of the precision laser goniometer system is presented in Fig. 1. The RL, the OAS rotor and the polyhedral prism are mounted on the spindle of the aerostatic bearing. The OAS stator and the null indicator, optically connected with the polyhedral prism, are mounted on the immovable housing of the system. The drive implements the rotation of the spindle with quasi-constant velocity. The output signals of the RL, the OAS and the null indicator are passed through appropriate signal shapers, SRL, SOAS, and SNI, and arrive at the interface I that carries out the preliminary data processing and transfer to the personal computer PC.

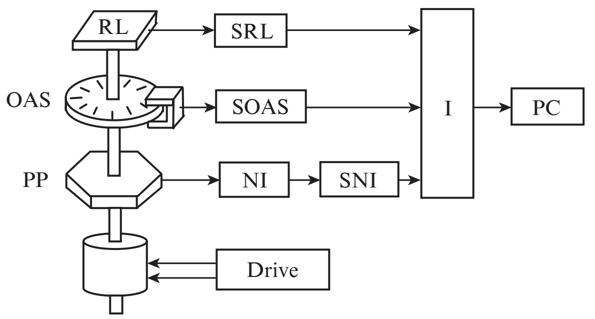

Figure 1. Functional diagram of the precision laser goniometer system.

In the present scheme the main angle transducers are the RL and the OAS. The polyhedral prism and the null indicator perform the secondary function and are intended for transferring the angle unit to the reference devices.

3. Study of systematic error components

As known [6], the angle, measured with the RL, is given by the expression

$$\varphi_{ikj} = 2\pi \frac{N_{\varphi_{ikj}} \pm F' t_i}{N_{2\pi_{kj}} \pm F' T}, \tag{1}$$

where N_φ and $N_{2\pi}$ are the numbers of periods (pulses) of the RL output signal in the measurement interval of the angle φ and in the interval 2π, respectively; T is the revolution period; F' is the RL generalised null shift; t_i is the time of the angle measurement; i is the number of the measured angle; k is the number of the RL angular position with respect to the spindle; and j is the revolution number.

The result of measuring the ith angle in the system under consideration is calculated as the value of the measurement results, averaged over 16 revolutions of the shaft, when the RL is in one of the positions, fixed with respect to the shaft (k = const), after subtraction of the RL systematic error s_i^{RL}:

$$\varphi_i = \frac{1}{16}\sum_{j=1}^{16} \varphi_{ij} - s_i^{\mathrm{RL}}. \tag{2}$$

The measuring scheme, presented in Fig. 1, was experimentally studied using a test mock-up of the precision laser goniometer system.

Figure 2 shows the results of OAS calibration (the first part of the cross-calibration procedure), implemented by means of the RL. In the process of calibration the output signal from the OAS (342 000 scale labels per revolution) was passed through the counting frequency divider with the division coefficient 900. The division resulted in the reduction of the number of output pulses to 360 per a complete revolution, i.e., the nominal angle between the pulses after the divider was 1°. The data were obtained for different positions of the RL with respect to the rotor of the measuring setup, i.e., the operations, necessary for implementation of cross-calibration, were carried out. The angles of sequential turns of the RL with respect to the rotor amounted to 60° (six different positions of the RL).

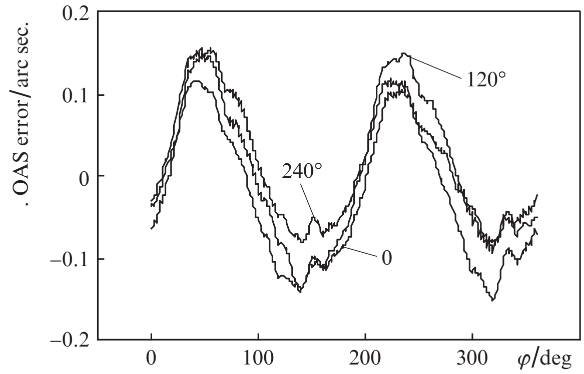

Figure 2. The results of OAS calibration at different angular positions of the RL with respect to the rotor of the system.

Figure 2 presents the results for three (of six) angles of the RL turn, namely, 0, 120°, and 240°. As mentioned above, the appropriate processing of data allows determination of systematic errors, introduced by the RL and OAS. The OAS systematic error δ_i^{OE} is found by simple averaging of the six obtained dependences $\delta_i^{\mathrm{OE}}(\varphi)$ and subtracting the nominal values of the angles φ_i^{nom}:

$$\delta_i^{\mathrm{OE}} = \frac{1}{16 \times 6} \sum_{k=1}^{6} \sum_{j=1}^{16} \varphi_{ikj} - \varphi_i^{\mathrm{nom}}. \tag{3}$$

The result of such averaging is presented in Fig. 3. It is seen that the systematic error of the OAS is concentrated in the second harmonic of the rotation frequency, and the amplitude of this harmonic amounts to $\sim 0.12''$.

The RL systematic error was determined by subtracting the averaged systematic error of the OAS from the systematic errors of the OAS for each position of the RL. Each of the six

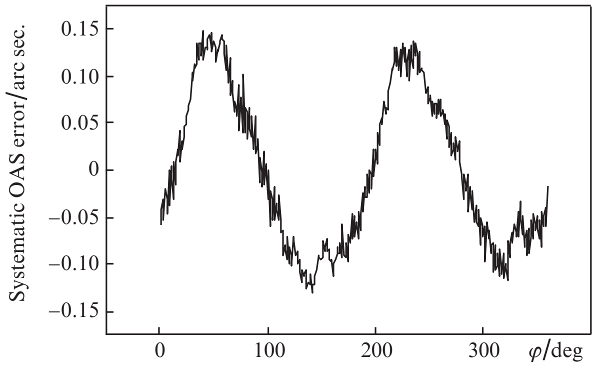

Figure 3. Systematic OAS error.

curves, obtained after such subtraction, represents the systematic error of the RL and has its own phase, determined by the position of the RL with respect to the rotor of the measuring setup in the current measurement. Averaging over all six curves was performed after the appropriate phase shift of each curve. This procedure is described by the expression

$$\delta_i^{\mathrm{RL}} = \frac{1}{6}\sum_{k=1}^{6}\Delta\varphi_{i+(k-1)60,k}, \tag{4}$$

where

$$\varphi_{ik} = \frac{1}{16}\sum_{j=1}^{16}\Delta\varphi_{ikj} - \delta_i^{\mathrm{OE}}.$$

The result of such data processing is presented in Fig. 4. It is seen, that the RL systematic error with the amplitude ~0.016″ is concentrated in the first harmonic of the rotation frequency.

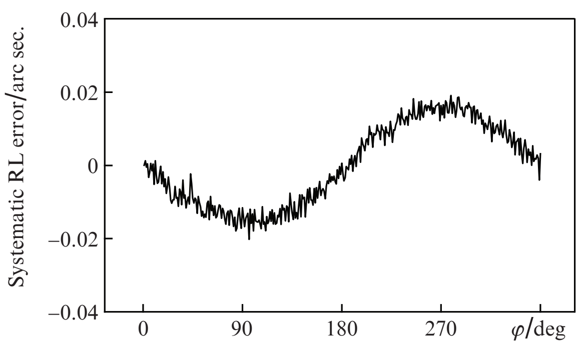

Figure 4. Systematic error of RL.

The dependence of the first harmonic amplitude of the RL systematic error upon the velocity of rotation is presented in Fig. 5. It is seen that the amplitude linearly grows with increasing the revolution time. The proportionality coefficient is equal to $0.0064 \pm 0.0003''\,\mathrm{s}^{-1}$. The observed dependence is determined by the influence of the external magnetic field on the RL particular type GL-1 [5]. In the stationary conditions, under which the precision laser goniometer system should operate, the compensation of the RL systematic error is possible.

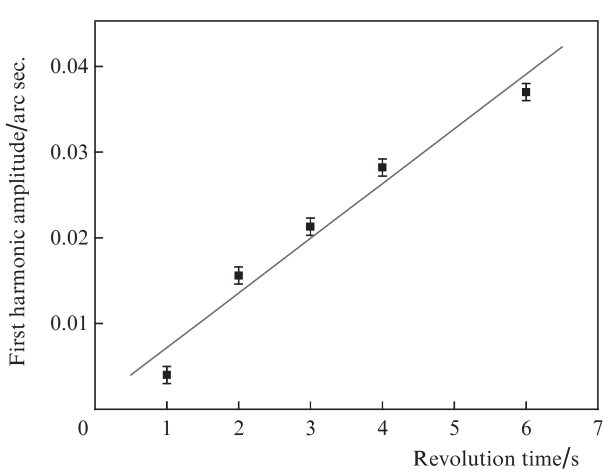

Figure 5. Dependence of the first harmonic amplitude of the RL systematic error on the velocity of RL rotation.

Thus, it is possible to conclude, that under the conditions of sufficient magnetic insulation of the setup the residual systematic error of the angle measurement does not exceed 0.01″.

4. Study of the random error of angle measurements

4.1. Statistical distribution of the results of measurements

Consider the determination of the random component of the error. The random error is defined by the value of the sample root mean square deviation

$$\sigma_{ik} = \left[\frac{1}{15\times 16}\sum_{j=1}^{16}(\varphi_{ijk} - \varphi_{ik})^2\right]^{1/2} \tag{5}$$

and the fractile of distribution of the sample mean of the measurement results.

To estimate the confidence intervals, in which the results of the angle measurements lie, one should know the distribution function of their random errors, as well as the confidence intervals, in which the systematic errors lie. The solution of this problem may be found by means of statistical and correlation analysis of the conditions, under which the measurements are performed.

To carry out the statistical analysis, let us write the formula for the measured angle φ in the form:

$$\varphi = 2\pi\frac{N_\varphi}{N_{2\pi}}.$$

The readout of the number N of the output signal periods by the counter begins at the moment $t = 0$ of starting the measurement, at the moment $t = t_\varphi$ we get the value N_φ, and at the moment $t = T$ of completing the rotor revolution we get the value $N_{2\pi}$. Fixing of these time moments is locked to the fronts of the OAS output signal.

The information about the angular position of the OAS rotor and the RL base is contained in the current values of the phases of output signals from the angle sensors, included in the measuring system. Therefore, the main sources of a random error are random processes, describing phase noises of the signals, output from the RL and OAS and having different statistical characteristics.

The fluctuations of the RL output signal phase are caused, first, by random fluctuations of the signal frequency (which may be presented as a stationary broad-band random process), due to spontaneous radiation of the active medium. Since during a complete revolution of the platform a large enough number of spontaneous emission events occurs, each of them equally affecting the number of periods of the RL output signal, in correspondence with the central limit theorem of the probability theory [16] the law of distribution of the number of periods of this signal may be considered normal. The Wiener process is usually chosen as a model of the random process, describing the random deviations of the number of periods of the RL output signal. The numbers of periods of the output signal N_φ and $N_{2\pi}$ in the intervals $[0, t_\varphi]$ and $[t_\varphi, T]$ are not correlated. The random error of formation of the measured angle boundary is caused by the shot noises of the photodetector and the thermal noises of the OAS output signal formation tract. The white Gaussian noise may be used as a model of this error.

Based on these considerations, the 2D distribution $f_2(N_\varphi, N_{2\pi})$ of the number of periods N_φ and $N_{2\pi}$ may be assumed normal and presented in the form

$$f_2(N_\varphi, N_{2\pi}) = \frac{1}{2\pi\sigma_1\sigma_2\sqrt{1-r^2}} \exp\left\{-\frac{1}{1(1-r^2)} \times\left[\frac{(N_\varphi - a_1)^2}{\sigma_1^2} - \frac{2r(N_\varphi - a_1)(N_{2\pi} - a_2)}{\sigma_1\sigma_2} + \frac{(N_{2\pi} - a_2)^2}{\sigma_2^2}\right]\right\},$$

where a_1 and a_2 are the mean values of N_φ and $N_{2\pi}$, respectively; σ_1 and σ_2 are their root mean square deviations; and r is the correlation coefficient for N_φ and $N_{2\pi}$.

Consider the distribution function of the result of a single angle measurement $f(\varphi)$. The analysis of Eqn (1) shows that $f(\varphi)$ can be expressed in terms of the 2D distribution function $f_2(N_\varphi, N_{2\pi})$ in a following way:

$$f(s) = \int_{-\infty}^{\infty} f_2(su, u)\,|u|\,\mathrm{d}u = \frac{\sqrt{1-r^2}}{\pi} \frac{\sigma_1\sigma_2}{\sigma_1^2 - 2r\sigma_1\sigma_2 s + \sigma_2^2 s^2} \times \exp\left[-\frac{1}{2(1-r^2)\sigma_1^2\sigma_2^2}\left| a_2^2\sigma_1^2 - 2ra_2a_1\sigma_1\sigma_2 + a_1^2\sigma_2^2\right|\right] \times\left[1 + \sqrt{2\pi}\,z\exp(z^2/2)\,\Phi_0(z)\right], \qquad (6)$$

where $s = \varphi/2\pi = N_\varphi/N_{2\pi}$ (the result of measurement expressed in complete revolutions of the shaft);

$$z = \frac{a_2\sigma_1^2 - ra_1\sigma_1\sigma_2 + a_1\sigma_2^2 s - ra_2\sigma_1\sigma_2 s}{\sigma_1\sigma_2\sqrt{(1-r^2)(\sigma_1^2 - 2r\sigma_1\sigma_2 s + \sigma_2^2 s^2)}};$$

$\Phi_0(x)$ being the Laplace function. For the case of the shaft uniform rotation in the approximation of white Gaussian noise for the fluctuations of the RL output signal frequency, the distribution parameters are expressed as [4]:

$$a_1 = N_\varphi,\ a_2 = N_{2\pi},\ \sigma_1^2 = K^2(R_{\mathrm{dr}}^2 T\langle s\rangle + 2D_{\mathrm{OE}}),$$

$$\sigma_2^2 = K^2(R_{\mathrm{dr}}^2 T + 2D_{\mathrm{OE}}),$$

$$r = \left[\frac{(R_{\mathrm{dr}}^2 T\langle s\rangle + D_{\mathrm{OE}})^2}{(R_{\mathrm{dr}}^2 T\langle s\rangle + 2D_{\mathrm{OE}})(R_{\mathrm{dr}}^2 T + 2D_{\mathrm{OE}})}\right]^{1/2},$$

where R_{dr} is the coefficient of random drift of the RL; $K = N_{2\pi}/2\pi$ is the scale factor of the RL; D_{OE} is the random variance of the OAS error for one limit of the angular interval.

Practically we deal with the limit case of small fluctuations, i.e., $\sigma_1, \sigma_2 \ll N_\varphi, N_{2\pi}$. In this case from the initial equation (1) we get the relation

$$s = s_0 + \delta s = \frac{\langle N_\varphi\rangle + \delta N_\varphi}{\langle N_{2\pi}\rangle + \delta N_{2\pi}} \approx \frac{\langle N_\varphi\rangle}{\langle N_{2\pi}\rangle}\left(1 + \frac{\delta N_\varphi}{\langle N_\varphi\rangle} - \frac{\delta N_{2\pi}}{\langle N_{2\pi}\rangle}\right).$$

The random variable δs is presented in the form of algebraic sum of two random quantities $\delta N_\varphi/\langle N_\varphi\rangle$ and $\delta N_{2\pi}/\langle N_{2\pi}\rangle$, distributed according to the normal law. From here it follows that the quantity s is also distributed according to the normal law:

$$f(s) = \frac{1}{\sqrt{2\pi D_s}} \exp\left[-\frac{(s - \langle s\rangle)^2}{2D_s}\right].$$

For the results of a single angle measurement we get

$$f(\varphi) = \frac{1}{\sqrt{2\pi D_\varphi}} \exp\left[-\frac{(\varphi - \langle\varphi\rangle)^2}{2D_\varphi}\right], \qquad (7)$$

where the variance of the measured angle is

$$D_\varphi(\langle\varphi\rangle) = \begin{cases} D_{\mathrm{OE}}(0) + D_{\mathrm{OE}}(\langle\varphi\rangle) \\ +\left[R_{\mathrm{dr}}^2 T - 2D_{\mathrm{OE}}(0)\right]\left(\dfrac{\langle\varphi\rangle}{2\pi}\right)\left(1 - \dfrac{\langle\varphi\rangle}{2\pi}\right), & \langle\varphi\rangle \neq 0, 2\pi, \\ 0, & \langle\varphi\rangle = 0, 2\pi. \end{cases} \qquad (8)$$

Based on the results of the analysis, one can draw a conclusion that in order to estimate the mean values of measurement results and to construct the appropriate confidence intervals it is necessary to use the Student distribution and χ^2 distribution.

It is worth noting that the distributions over the unlimited rotation angle, presented above, are a mathematical abstraction, since in the laser goniometer the application of the self-calibration algorithm restricts the operation range of the measurements to the values within the interval $[0, 2\pi]$. Commonly, the calibration of the digital angle transducers is also performed within the same range of angles. In these cases the so called wrapped distributions [17] are used.

In the case of small fluctuations the distribution is reduced to the wrapped normal one, which can be calculated using ζ-functions:

$$f(\varphi) = (2\pi)^{-1}\zeta_3(\varphi - \langle\varphi\rangle, \rho),$$

where $\rho = \exp(-D_\varphi)$, and the values of ζ_3 are tabulated in [18]. In the limit case $\sqrt{D_\varphi}/\varphi \ll 1$ it is still possible to use the standard normal distribution.

The parametric dependence of the probability density distribution on the measured angle is presented in Fig. 6. When the value of the measured angle approaches the edges of the self-calibration interval $(0, 2\pi)$ the variance decreases in correspondence with Eqn (8) and the maximal probability density increases. At the edges of the self-calibration interval the probability density distribution degenerates into a delta-function.

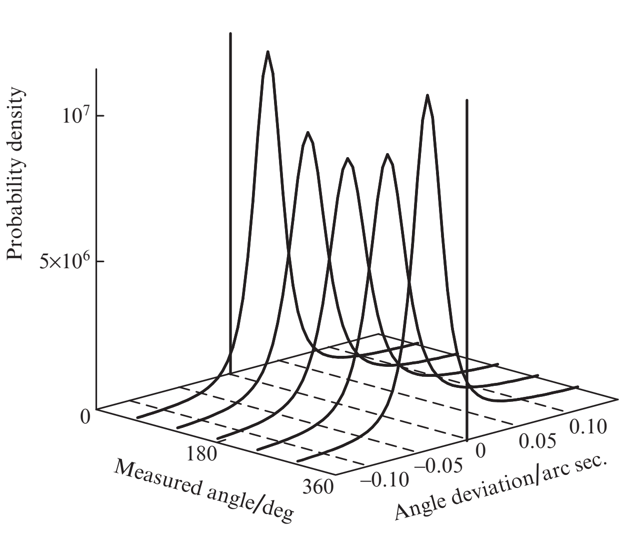

Figure 6. Parametric dependence of the probability density distribution on the measured angle.

The sample distributions, obtained using the measuring setup in the dynamic regime, are presented in Fig. 7 (the histogram and the approximation by a Gaussian curve). Figure 8 shows the histogram of the distribution of RL scale factors, obtained using the interference null indicator, which characterises the RL as an angle sensor with the extremely uniform scale.

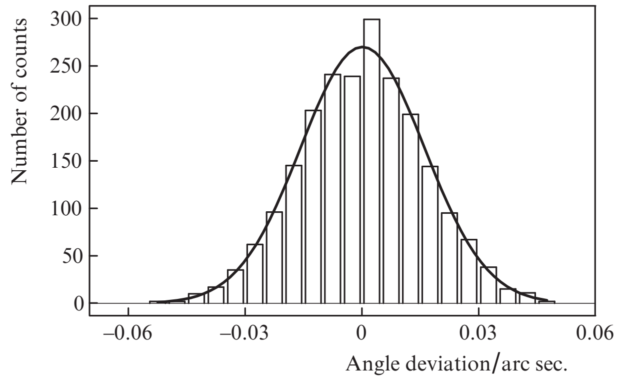

Figure 7. Error histogram of the angular measurements and its approximation by a Gaussian curve.

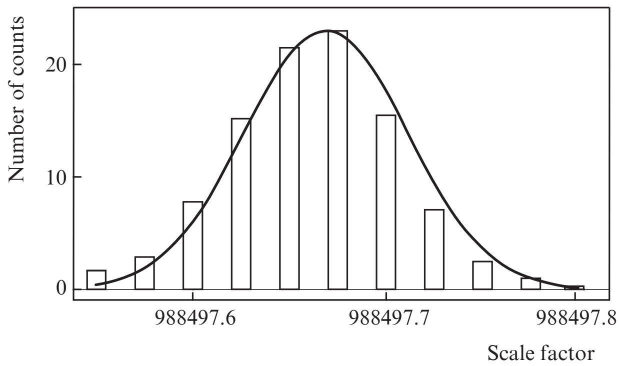

Figure 8. Histogram of distribution of RL scale factor and its approximation by a Gaussian curve.

4.2. The technique of separate estimation of random errors, introduced by the rind laser and the OAS

In the process of measurements the data that serve for estimating the result are integer values, read from the counters of complete periods of the RL output signal. The value and the statistical properties of the random error of measuring a certain angle φ are determined by the measurement time t_φ, the statistical characteristics of the RL output signal frequency and phase, and the statistical characteristics of the angle sensor signal.

To separate the components of the random error, introduced by the RL and the OAS, the parametric dependence (8) is used. The typical plot of this dependence is presented in Fig. 9.

Let us write the expression (8) in the form of decomposition in terms of two functions, $F_1(s)$ and $F_2(s)$:

$$D_\varphi(s) = \beta_1 F_1(s) + \beta_2 F_1(s), \qquad (9)$$

where $F_1(s) = s(1 - s)$ and $F_2(s) = s^2 - s + 1$ are two independent, but not orthogonal polynomials of the same power,

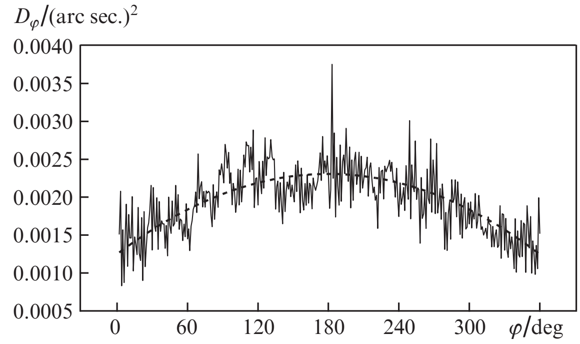

Figure 9. Dependence of the measurement result on the measured angle. The dashed line plots the approximation by Eqn (8).

which will represent two independent variables in the linear regression procedure; $\beta_1 = R_{\rm dr}^2 T$ and $\beta_2 = 2D_{\rm OE}$ are the linear regression coefficients (the time dependence of $D_{\rm OE}$ is not considered here); $s = \varphi/2\pi$.

As a result of calculating the dependence of variance upon the rotation angle for the values s_i, we get the sample $D_{\varphi i}$ ($i = 1, \ldots, m$, where m is the sample volume). According to [19], we assume $D_{\varphi i} = D_\varphi(s_i) + \nu_i \equiv y_i$, where the random variable ν_i is centred and obeys a normal distribution. The equations of linear regression of the random variables y_i (i.e., $D_{\varphi i}$) with respect to independent variables $z_{1i} = F_1(s_i)$ and $z_{2i} = F_2(s_i)$ in vector form are presented as

$$My_i = \boldsymbol{\beta}^{\rm t} \boldsymbol{Z}_i,$$

where

$$\boldsymbol{Z}_i = \begin{pmatrix} z_{1i} \\ z_{2i} \end{pmatrix}$$

is the vector of independent variables;

$$\boldsymbol{\beta} = \begin{pmatrix} \beta_1 \\ \beta_2 \end{pmatrix}$$

is the vector of regression coefficients; M is the operator of calculating the mathematical expectation of a random variable; the superscript t denotes the transpose of a matrix or a vector.

As a result of performing the regression, we get the estimate

$$\boldsymbol{b} = \begin{pmatrix} \beta_1 \\ \beta_2 \end{pmatrix}$$

of the vector $\boldsymbol{\beta}$, which is a solution of the normal equations $A\boldsymbol{b} = \boldsymbol{c}$, where

$$A = \sum_{i=1}^{m} \boldsymbol{Z}_i \boldsymbol{Z}_i^{\rm t}$$

is the non-degenerate matrix of the system of normal equations and

$$\boldsymbol{c} = \sum_{i=1}^{m} y_i \boldsymbol{Z}_i.$$

The vector $\boldsymbol{b} = A^{-1}\boldsymbol{c}$ minimises the sum

$$\sum_{i=1}^{m} (y_i - \tilde{\boldsymbol{b}}^{\rm t} \boldsymbol{Z}_i)^2$$

on the set of all p-dimensional vectors $\tilde{\boldsymbol{b}}$ and represents an estimate within the least-squares procedure. For independent and normally distributed variables $y_1, ..., y_m$ the estimate $\boldsymbol{b}$ is distributed according to the multidimensional normal law $F(\boldsymbol{\beta}, \sigma^2 A^{-1})$, and the estimate of $(m-p)\tilde{\sigma}^2/\sigma^2$ has the distribution χ^2 with the number of degrees of freedom $m-p$, where $p=2$ is the number of regression coefficients. The unbiased estimate $\tilde{\sigma}$ of the root-mean-square error σ can be found from the relation

$$(m-2)\tilde{\sigma}^2 = \sum_{i=1}^{m}(y_i - \boldsymbol{b}^{\mathrm{t}}\boldsymbol{Z}_i)^2.$$

Based on the mentioned distribution laws, one can obtain the confidence intervals for individual components of the vector $\boldsymbol{b}$. Thus, if we are interested in the component β_l ($l = 1, 2$), then the quantity $(b_l - \beta_l)(\tilde{\sigma}\sqrt{a^{ll}})^{-1}$ has a t-distribution with $m-p$ degrees of freedom. Specifying the value of the confidence probability P, we arrive, according to [19, 20], at the following expression of the confidence interval for the regression coefficient β_l:

$$b_l - \tilde{\sigma}\sqrt{a^{ll}}\, t_{(1-P)/2} \leqslant \beta_l \leqslant b_l + \tilde{\sigma}\sqrt{a^{ll}}\, t_{(1-P)/2}, \quad (10)$$

where $a^{ll} = (A^{-1})_{ll}$ are the diagonal elements of the normalised correlation matrix of the estimate vector $\boldsymbol{b}$.

Let us obtain the confidence interval bounds for the regression coefficients β_1 and β_2, as well as for the root-mean-square random error of the OAS, $\sigma_{\mathrm{OE}} = \sqrt{\beta_2}$, and the coefficient of random drift of the RL, $R_{\mathrm{dr}} = \sqrt{\beta_1/T}$:

$$\left[b_2 - \tilde{\sigma}\sqrt{a^{22}}\, t_{(1-P)/2}\right]^{1/2} \leqslant \sigma_{\mathrm{OE}} \leqslant \left[b_2 + \tilde{\sigma}\sqrt{a^{22}}\, t_{(1-P)/2}\right]^{1/2},$$
$$\frac{1}{\sqrt{T}}\left[b_2 - \tilde{\sigma}\sqrt{a^{11}}\, t_{(1-P)/2}\right]^{1/2} \leqslant R_{\mathrm{dr}} \leqslant \frac{1}{\sqrt{T}}\left[b_2 + \tilde{\sigma}\sqrt{a^{11}}\, t_{(1-P)/2}\right]^{1/2}, \quad (11)$$

where

$$a^{ll} = \frac{1}{\Delta}\sum_{i=1}^{m} F_{3-l}^2(s_i);$$

$$\Delta = \sum_{i=1}^{m} F_1^2(s_i) \sum_{i=1}^{m} F_2^2(s_i) - \left[\sum_{i=1}^{m} F_1(s_i) F_2(s_i)\right]^2.$$

Using the data, presented in Fig. 9 for $P = 0.95$ ($t_{0.025} = 1.96$), we get, according to (10, (11), the numerical estimates for root-mean-square random error of the OAS, σ_{OE}, and the random drift coefficient of the RL, R_{dr}:

$$0.034'' \leqslant \sigma_{\mathrm{OE}} \leqslant 0.036'',$$

$$0.042''/\sqrt{\mathrm{c}} \leqslant R_{\mathrm{dr}} \leqslant 0.044''/\sqrt{\mathrm{c}}.$$

Based on the results of the performed analysis, one can estimate the unrecorded systematic error θ and the random error of the angle measurement. As an estimate of one of the components of unrecorded systematic error we take the half-width of the confidence interval for the estimation of the systematic OAS error, which is determined by the maximal value of the variance of the random measurement error (8) with the number of revolutions $m_{\mathrm{rev}} = 16$ and the number of repeated measurements $n_{\mathrm{pos}} = 6$ at different positions of the RL: $\theta_{\mathrm{OE}} = \sqrt{D_\varphi(\pi)/(m_{\mathrm{rev}} n_{\mathrm{pos}})}\, t_{0.025} = 0.01''$. The systematic error component, caused by the influence of the Earth's magnetic field on the RL, is estimated as $\theta_{\mathrm{RL}} = 0.016'' \pm 0.001''$.

As an estimate of the root-mean-square random error we assume $\sigma = \sqrt{D_\varphi(\pi)/m_{\mathrm{rev}}} = 0.013'' \pm 0.001''$ at $T = 2$ s, which corresponds to the maximal random error of the RL.

5. Implementation of precision laser goniometer schemes

The considered concept of constructing high-accuracy laser goniometer systems was implemented in a number of setups, among which one should mention the standard system of the plane angle unit for rigid rotations and the measuring and computing complex for automated control of high-capacity digital angle transducers.

5.1. The standard system of the plane angle unit for rigid rotations

The system enters the State Primary Standard GET 94-01, intended for reproduction, storage and transfer of the unit of rigid body linear acceleration and the unit of plane angle for rigid angular motion. The standard comprises a number of standard systems, including the standard rotation system NTS-3, implementing the method of turning a rotary platform in the gravitational field of the Earth and the goniometric method. The rotational system NTS-3 reproduces the unit of linear acceleration in the frequency range 0.05–30 Hz and the amplitude range 10^{-4}–10 m s^{-2} and the unit of plane angle for the angular displacement of a rigid body within the range 0.2″–360°.

Figure 10 presents a simplified block diagram of the NTS-3 setup. The system operates in two regimes, the regime of reproducing variable low-frequency accelerations and the regime of reproducing variable plane angles.

The reproduction of an angle at the base velocity (0.5 revolutions per second) was implemented using the rotating RL, in which the phase of the output signal is proportional to the angle of rotation. The use of a holographic angle sensor in the setup allows implementation of angle transfer in the extended

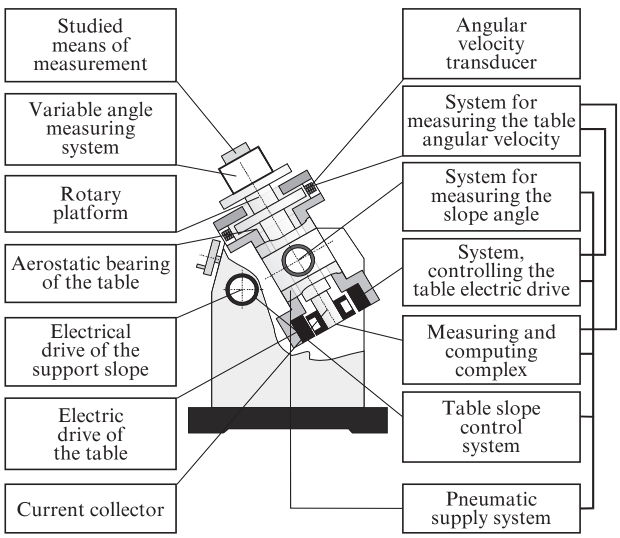

Figure 10. Block diagram of the NTS-3 setup with the standard system of the plane angle unit.

range of rotation velocities and determination of errors, introduced by both sensors. The polyhedral prism and the null indicator play the secondary role and are intended for transferring the value of the angle unit to the standards of the next rank and working measuring instruments, as well as for comparison with the State Primary Standard of the unit of plane angle GET 22-80.

The results of comparison of the standard GET 94-01 of the plane angle unit for angular displacement of a rigid body with the standard of the plane angle unit GET 22-80 using the 12-face prism are presented in Table 2. It is seen that the difference in results, obtained with the use of two angle standards, does not exceed 0.03″, except for the central angle between the sixth and the seventh face.

Table 2. The results of intercomparison of standards GET 94-01 and GET 22-80.

Face number	Measured deviation from the nominal value (″) (GET 94-01)	Root-mean-square deviation of the measurement results (″)	Actual deviation from the nominal value (″) (GET 22-80)
1-2	−1.63	0.01	−1.60
2-3	1.58	0.01	1.56
3-4	−0.89	0.03	−0.89
4-5	−0.56	0.01	−0.54
5-6	−0.13	0.02	−0.12
6-7	0.37	0.02	0.26
7-8	−1.34	0.03	−1.32
8-9	1.79	0.03	1.76
9-10	−0.03	0.01	0.04
10-11	0.46	0.02	0.49
11-12	0.29	0.02	0.31
12-1	0.08	0.01	0.05

Thus, the intercomparison of standards has proved reliability of the results of the study of the NTS-3 standard system, as well as the fact that this system allows transfer of the size of angle unit with the use of a RL or OAS. It is worth noting that the OAS possesses greater long-term stability, as compared with the RL. The systematic error of the OAS essentially depends on the mutual localisation of reading heads and the scale and is subject to the influence of thermodynamic factors and deformation processes. For RLs the systematic error is smaller, and its sources are external magnetic fields. Therefore, for high-accuracy measurements it is preferable to use RLs. At the same time, for RLs the range of measured angular velocities is limited (usually $\pi/6-2\pi$ rad s^{-1}), while for OAS it is wider. For RL the lower bound of the range is determined by physical processes in the laser (capture of contradirectional mode frequencies), while for the OAS the range is determined by the parameters of the used optoelectronic components. To provide the maximal accuracy it is reasonable to perform the cross-calibration procedure directly before the measurements.

5.2. Measuring and computing complex for automated control of high-capacity digital angle transducers

The measuring and computing complex (MCC) is intended for automated control of high-capacity digital angle transducers (DATs). The MCC provides the measurement of the basic characteristics of DATs within the angle range 0–360°, angular velocities $\pm(30-720)°\ s^{-1}$, and angular accelerations $\pm(0-20)°\ s^{-2}$ with the error not exceeding 0.05″.

According to its metrological characteristics, the MCC can be rated among the standards of the first class [21], which makes great demands of the operation conditions, as well as the choice of the methods and means of testing the complex, aimed at confirmation of its metrological characteristics.

To obtain the characteristics mentioned above, in the MCC they use the principle, accepted in the standard of the angle unit for angular displacement of a rigid body, i.e., integration of the RL and OAS. In contrast to GET 94-01, in the MCC the role of the main angle sensor, which is used to measure the angular parameters of the DAT code change, is played by the OAS. The RL serves to keep the plane angle unit and to determine the systematic error of the OAS at the base velocity.

Figure 11 presents the functional diagram of the MCC. The complex consists of the electromechanical system, the controlling system, the optoelectronic measuring system and the system of displaying the information.

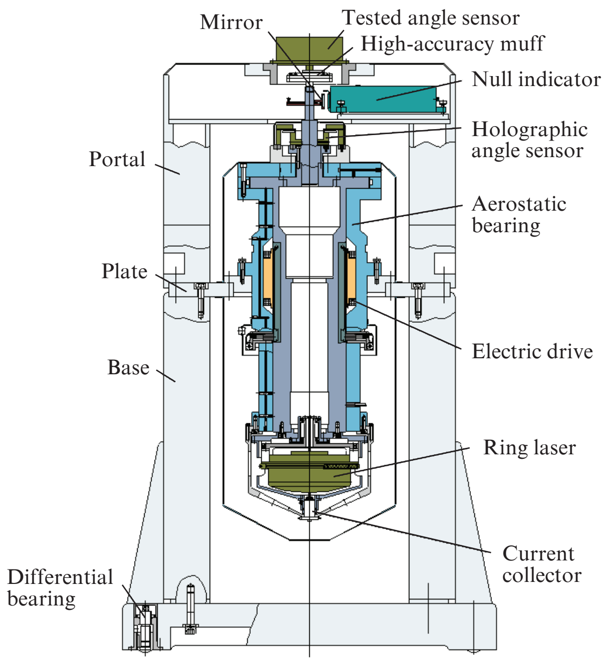

Figure 11. Functional diagram of MCC for control of high-capacity digital angle transducers.

The MCC operation principle consists in comparing the values of rotation angle of the rotary platform obtained using the OAS and the studied DAT at the same moment of time. The signals from DAT pass through the interface device and arrive at the electronic unit of the MCC. Simultaneously, the signals from the OAS arrive at this unit. On request signals, produced by the studied DAT or the null indicator, the information about the rotation angle of the OAS and DAT is recorded by the board of information processing and transfer [22] and then passed to the computer for further processing and output of the result to monitor, printer, or hard disc.

The error of the MCC at the base velocity is defined as the difference between the results of measuring the characteristics of OAS by the RLs, that enter into the composition of the MCC, and the master setup HTS-3 (as a part of the standard GET 94-01). We should note that the present work is the first one in which the transfer of the plane angle unit from the GET 94-01 standard to the measuring instrument was implemented using RL.

The result of the MCC error determination at the base velocity is presented in Fig. 12. The harmonic analysis has shown that the resulting error involves second, third and fourth ‘revolution’ harmonics that characterise the uneliminated systematic error. The uneliminated systematic component of the error does not exceed 0.03″, and the random components have the root-mean square value of 0.008″.

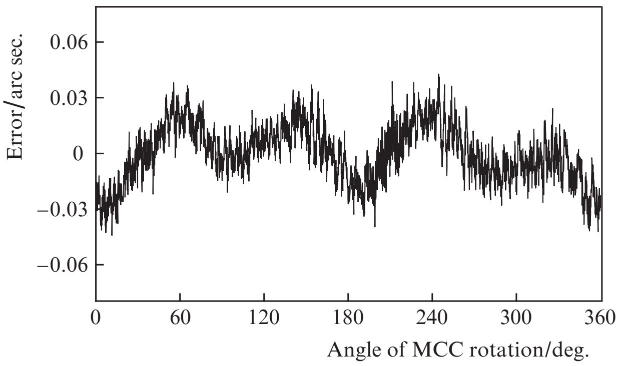

Figure 12. MCC error at the base velocity.

6. Conclusions

The obtained results demonstrate high potentialities of using the systems, based on integrating RLs with high-accuracy angle sensors, especially those, in which the holographic method of angle scale recording is implemented. Precision laser goniometer systems, based on the concept considered here, provide the performance of angular measurements with the systematic component of the error less than 0.01″ and nearly the same random component. Naturally, the presented estimates do not include the additive errors of the means, intended for the angle unit size transfer, such as the optical null indicator, the muff, etc. Further enhancement of angular measurement accuracy implies, on the one hand, increasing the resolving power and long-term stability of the RL and OAS characteristics and, on the other hand, improvement of the auxiliary means of transferring the size of the angular unit.

References

1. *Proc. 186th PTB-Seminar* (Braunschweig, 2003).
2. Just A., Krause M., Probst R., Wittekopf R. *Metrologia*, **40**, 288 (2003).
3. Filatov Yu., Loukianov D.P., Probst R. *Metrologia*, **34**, 343 (1997).
4. Burnashev M.N., Loukianov D.P., Pavlov P.A., Filatov Yu.V. *Kvantovaya Elektron.*, **30**, 141 (2000) [*Quantum Electron.*, **30**, 141 (2000)].
5. Krivtsov E.P., Filatov Yu.V. *Izmeritel'naya tekhnika*, (12), 11 (1989).
6. Pavlov P.A. *Izmeritel'naya tekhnika*, (1), 17 (2008).
7. Gordeev S.V., Turukhano B.G. *Opt. Laser Technol.*, **28**, 255 (1996).
8. Sim P.J., in *Modern Techiques in Metrology*. Ed. by P.L. Hewitt (Singapore, World Scientific, 1984) pp 102–121.
9. Smirnov V.A. et al. *Izmeritel'naya tekhnika*, (4), 7 (1991).
10. Glagolev I.P. et al. *Izmeritel'naya tekhnika*, (4), 8 (1991).
11. Masuda T., Kajitani V. *J. Robotics Mechatronics*, **5**, 448 (1993).
12. Watanabe T. et al. *Proc. SPIE Int. Soc. Opt. Eng.*, **4401**, 267 (2001).
13. Just A. et al. *Metrologia*, **40**, 288 (2003).
14. Probst R. *Meas. Sci. Technol.*, **18**, 1 (2007).
15. Burnashev M.N., Krivtsov E.P., Pavlov P.A., Filatov Yu.V. *Materialy mezdunar. nauchno-tekhn. konf. ‘Nauka, obrazoveniye i obschestvo v 21 veke’* (Proc. Int. Sci. Techn. Conf. ‘Science, Education and Society in the 21th Century’) (Saint-Petersburg, 2006) p. 160.
16. Levin B.R. *Teoreticheskiye osnovy statisticheskoy radiotekhniki* (Theoretical Foundations of Statistical Radio Engineering) (Moscow: Radio i Svyaz', 1989).
17. Mardia K. *Statistics of Directional Data* (New York: Academic Press, 1972).
18. Shuler M., Gebelin H. *Five Place Table of Elliptical Function Based on Jacobi's Parameter q* (Berlin: Springer, 1955).
19. Anderson T.W. *The Statistical Analysis of Time Series* (New York: John Wiley and Sons, 1971).
20. Himmelblau D.M. *Process Analysis by Statistical Methods* (New York: John Wiley and Sons, 1970).
21. GOST 8.577-2002. *Gosudarstvennaya poverochnaya schema dlya sredstv izmereniy lineynykh uskoreniy i ploskogo ugla pri uglovom peremeschenii tverdogo tela* (State Standard 8.577-2002. State measurement chain for means of measuring linear accelerations and plane angle at angular displacement of a rigid body).
22. Grushvitskii R.I., Kilochek D.V., Pavlov P.A. *Izv. SPbGETU ‘LETI’*, (1), 64 (2008).